EFDA–JET–PR(13)17

E. Joffrin, M. Baruzzo, M. Beurskens, Bourdelle, S. Brezinsek, J. Bucalossi, P. Buratti, G. Calabro, C.D. Challis, M. Clever, J. Coenen, E. Delabie, R. Dux, P. Lomas, E. de la Luna, P. de Vries, J. Flanagan, L. Frassinetti, D. Frigione, C. Giroud, M. Groth, N. Hawkes, J. Hobirk, M. Lehnen, G. Maddison, J. Mailloux, C.F. Maggi, G. Matthews, M. Mayoral, A. Meigs, R. Neu, I. Nunes, T. Puetterich, F. Rimini, M. Sertoli, B. Sieglin, A.C.C. Sips, G. van Rooij, I. Voitsekhovitch and JET EFDA contributors

Scenario Development at JET with the New ITER-like Wall

Scenario Development at JET with the New ITER-like Wall

E. Joffrin[1], M. Baruzzo[2], M. Beurskens[3], Bourdelle[1], S. Brezinsek[4], J. Bucalossi[1], P. Buratti[5], G. Calabro[5], C.D. Challis[3], M. Clever[4], J. Coenen[4], E. Delabie[6], R. Dux[7], P. Lomas[3], E. de la Luna[8], P. de Vries[9], J. Flanagan[3], L. Frassinetti[10], D. Frigione[5], C. Giroud[3], M. Groth[11], N. Hawkes[3], J. Hobirk[7], M. Lehnen[4], G. Maddison[3], J. Mailloux[3], C.F. Maggi[7], G. Matthews[3], M. Mayoral[12], A. Meigs[3], R. Neu[7], I. Nunes[13], T. Puetterich[7], F. Rimini[3], M. Sertoli[7], B. Sieglin[7], A.C.C. Sips[14], G. van Rooij[9], I. Voitsekhovitch[3] and JET EFDA contributors*

JET-EFDA, Culham Science Centre, OX14 3DB, Abingdon, UK

[1]IRFM-CEA, Centre de Cadarache, 13108 Sant-Paul-lez-Durance, France
[2]Conzorsio RFX Corso Stati Uniti 4 35127 Padova, Italy
[3]EURATOM-CCFE Fusion Association, Culham Science Centre, OX14 3DB, Abingdon, OXON, UK
[4]Association EURATOM/Forschungszentrum Juelich Gm bH 52425 Juelich Germany
[5]Associazione EURATOM-ENEA sulla Fusione, C.R. Frascati, Frascati , Italy
[6]Ecole Royale Militaire, Avenue de renaissance, 1000 Brussels, Belgium
[7]Max-Planck-Institut fur Plasmaphysik, Euratom Association, 85748, Garching Germany
[8]Laboratorio Nacional de Fusion, Asociacion EURATOM-CIEMAT, Madrid, Spain
[9]Association EURATOM/DIFFER, Rijnhuizen P.O. Box 1207 3430BE Nieuwegein, Netherlands
[10]Division of Fusion Plasma Physics, Association EURATOM-VR , KTH, SE-10044 Stockholm, Sweden
[11]Association Euratom-Tekes, VTT, PO Box 1000, 02 044 VTT, Finland
[12]EFDA-CSU, 85748 Garching bei München, Germany
[13]Instituto Superior Tecnico, 1049-001 Lisboa, Portugal
[14]JET-EFDA-CSU, Culham Science Centre, OX14 3DB, Abingdon, OXON, UK
** See annex of F. Romanelli et al, "Overview of JET Results", (24th IAEA Fusion Energy Conference, San Diego, USA (2012)).*

Preprint of Paper to be submitted for publication in
Nuclear Fusion

ABSTRACT:
In the recent JET experimental campaigns with the new ITER-like Wall (JET-ILW), major progress has been achieved in the characterisation and operation of the H-mode regime in metallic environment: i) plasma breakdown has been achieved at the first attempt and X-point L-mode operation recovered in a few days of operation, ii) stationary and stable type I ELMy H-modes with β_N~1.4 have been achieved in low and high triangularity ITER–like shape plasmas and are showing that their operational domain at H = 1 is significantly reduced with the JET-ILW mainly because of the need to inject large amount of gas (above 10^{22}D/s) to control core radiation. iii) in contrast the hybrid H-mode scenario has reached H factor of 1.2 to 1.3 at β_N of 3 for 2 to 3s. iv) in comparison to carbon equivalent discharges, total radiation is similar but the edge radiation is lower and Z_{eff} of the order of 1.3-1.4. At low gas fuelling rate (below 0.5 10^{22}D/s) and low ELM frequency (typically less than 10Hz), strong core radiation peaking is observed in H-mode discharges even when tungsten influx from the divertor is constant. High Z impurity transport from the plasma edge to the core appears to be the dominant factor to explain is paper reviews the major physics and operational achievements and challenges that an ITER-like wall configuration has to face to produce stable plasma scenarios with maximised performance.

1. INTRODUCTION

The transition to all metal plasma facing components is an essential step on the path to reactor scale fusion devices to minimise hydrogen fuel retention in the plasma facing components (PFCs) [1]. In this context, the JET ITER-like Wall (JET-ILW) with plasma-facing components made of beryllium in the main chamber and tungsten in the divertor was installed successfully in 2010/11 [2] to validate the first wall material mix for ITER. As a consequence, demonstrating the compatibility with the new JET-ILW of typical ITER scenarios such as the baseline or the advanced inductive H-modes (so called "hybrid") scenarios developed previously in a carbon environment has been one of the main line of the research of the 2011-2012 JET experimental campaign.

Stable H-mode baseline plasma (q_{95}~3, β_N~1.4) have been achieved in JET for about 5s up to a current of 3.5MA with a confinement factor H_{98y2} in the range of 0.7-0.9. Hybrid H-modes above $\beta_N = 3$ at $I_p = 2$MA (q_{95}~4, β_N~3) with and H_{98y2} factor exceeding 1.2 for 2s. Although operational issues such as the limited steady state heat load or the changes in plasma impurity composition were foreseen, the landscape of scenario operational domain has changed significantly and are consistent with the observation on other metallic devices such as ASDEX Upgrade [3] or C-MOD [4]. The most important results is that the access to H~1 confinement is in general much more restricted than with the carbon wall for the baseline H-mode scenario in both low ($\delta = 0.2$) and high shape ($\delta = 0.4$) mainly because of the need to control core radiation which was achieved by significant gas puffing rate. However, even with some gas puffing (~5.10^{21}e/s), H factor close to 1.3 can be reached in the advanced inductive (hybrid) H-mode scenario in JET with the JET-ILW.

The paper first presents an overview of the scenario performance with the JET-ILW and then

details the developments of the H-mode at high plasma current ($I_p = 3.5$MA) and at high normalised pressure ($\beta_N \sim 3$) referred to as the advanced inductive (hybrid) scenario [5]. Plasma composition, tungsten influx and core transport, the role of the ELMs and radiation patterns are important elements to be addressed and compared with the carbon wall in the discussion. In developing a fully integrated scenario, the main building blocks making a complete discharge from formation to current decay have also been studied experimentally. Current ramp up and down phases, H-mode termination and techniques for reducing the impact of disruption are also presented.

2. OVERVIEW OF THE H-MODE DEVELOPMENT IN JET WITH THE JET-ILW

In JET with the JET-ILW all the existing Carbon-fibre Composite (CFC) in direct contact with the plasma have been replaced with bulk beryllium as the predominant main chamber material and with tungsten surfaces in the divertor [2]. The divertor consists of thin (30 microns) W-coated CFC tiles and a single toroidally continuous belt of four-fold bulk tungsten tile at the outer strike point where the heat flux is expected to be the strongest [6]. The anticipated operating limits with the JET-ILW are most fundamentally driven by the relatively low melting point of beryllium (1356^{o}C), the limited robustness of tungsten coatings to slow and fast thermal cycles (operating temperature limited to 1200^{o}C) and the thermal capabilities of the support structures for the bulk tungsten tile limiting the energy dumped into the tile to typically 60MJ per stack. The protection of the JET-ILW was an integral part project from very early on and the surface temperature on the tiles (in particular the bulk tungsten tile used in general for the outer strike point of the magnetic configuration) has been systematically monitored during the step-wise increase of the power.

In the initial experimental phases with the JET-ILW, reliable breakdown conditions with pre-magnetisation of the primary current have been recovered in JET in the first discharge and even optimised to voltage of the order of what is expected in ITER (~0.25V.m) [7]. Series of identical limiter and X-point ohmic discharge have been carried out to establish the wall properties in constant plasma conditions [8]. First experiments have also shown that larger amount of gas (by typically a factor of 2 to 4) is required with the JET-ILW in the limiter phase for developing the discharge in the early phase of the current ramp-up phase so as to avoid either core impurity accumulation [9] or discharges sustained by slide-away electrons.

After this first step, stable Type I sawtoothing H-modes regime have been achieved in low and high triangular shaped magnetic configuration at 2.0MA/2.1T and then at 2.5MA 2.7T with $q_{95} = 3.3$ and neutral beam injection of typically 15MW of input power for 4 to 5s (Figure 1). During this initial development phase, metallic impurity events have been observed [10] but in the course of the further operation their frequency decreased steadily as the heating power was increased, suggesting either a conditioning effect of wetted surfaces by the plasma (metallic dust coming from the installation of the components) or a redistribution of the dust (consisting of W, Ni, Cr, Fe) in places of the vessel not receiving significant direct power flux. In these discharges, Z_{eff} is also substantially lower with the JET-ILW and a reduction from typically ~2 in the JET-C to ~1.3 in

the W-wall is generally achieved corresponding to a reduction of carbon content by a factor of 20 [1]. As a consequence, the dilution is also significantly less in these discharges than it was in the JET-C (typically 0.9-0.95 instead of 0.8), which is favourable for fusion born neutron production. In this early phase of H-mode operation [11], it became clear that significant amount of deuterium (rate above 10^{22}D/s) had to be puffed continuously during the main heating phase in order to achieve stable conditions in the H-mode phase and prevent central radiation peaking as already experienced in ASDEX Upgrade [12]. When lowering the gas fuelling rate, an increase of the bulk plasma radiation is observed from bolometry reconstruction often correlated with a collapse of the central temperature and the loss of sawteeth (Figure 2). This behaviour is also often correlated with an increase of the tungsten concentration in the plasma core as inferred from visible spectroscopy and soft X-ray emission. As the core radiation increases, the ELM frequency decreases, ELM-free phases increase in duration and this can eventually lead to a back transition to L-mode as the power across the separatrix P_{NET} decreases. Here, P_{NET} is defined as: $P_{NET} = P_{IN}$-dW/dt-$P_{RADBULK}$. (The last term is the total radiated power inside the last closed flux surface and P_{IN} the total input power). In these conditions, disruption by radiative collapse is less likely to occur if P_{IN} is maintained provided that heat deposition is located in the plasma centre (using ICRH for example) where the impurity and radiation peaking tend to occur possibly by neoclassical transport as observed in ASDEX Upgrade [13].

In JET, gas bleed had been used previously to increase the ELM frequency in the Carbon wall [14]. The increase of the power in H-mode regime also leads to an increase of the type I ELM frequency. The increase of the NBI power combined with strong deuterium gas puffing rate (in general above 10^{22}D/s) both helped to operate stable H-mode regime in JET with the JET-ILW by increasing the ELM frequency as it can be observed on figure 3. By scanning down the gas bleed with the JET-ILW, a minimum ELM frequency of typically 10Hz was found necessary to prevent excessive core plasma radiation peaking. The role of the ELM on core radiation control has also been observed in ASDEX Upgrade and the property they have to flush out tungsten evidenced [3]. Similar effect seems to be at play in the H-mode operation with the JET-ILW. However, it should be pointed out here that intra-ELM sputtering for 10Hz ELM was found to dominate inter ELM sputtering by almost one order of magnitude [15]. The increase of ELM frequency with the power could therefore compete with a possible stronger ELM-induced tungsten sputtering source.

In an attempt to open up the space for H = 1 and minimise the gas fuelling rate, vertical kicks [16] have been applied to control the ELMs at a given frequency larger than the natural frequency. Although the ELM frequency could indeed be controlled at about 20Hz and the gas rate minimised down to 5.10^{21} D/s (see figure 3), on the other hand, the confinement factor could not be restored to values H~1. More experiments are required to optimise the use of the kick technique (and also using pellet pacing [17]) to demonstrate the benefit of ELM pacing in the control of the core radiation. But these preliminary experiments are suggesting that ELM control has become a key element in the achievement of stable H-mode discharge in a metallic environment.

As it could be expected, the use of gas bleed can degrade the confinement of the H-mode (Figure 4a and 4b). At high triangularity (δ~0.4) the H-mode scenario shows a confinement degradation with gas puffing which was in general not observed with the JET-C [14]. Equivalent discharges with the same magnetic configuration at high triangularity 2.5MA/2.7T, using the same power and similar gas puffing rate (3 to 4 10^{22} e/s), show significantly lowered confinement with the JET-ILW (H_{98y2}~0.7) compared to JET-C (H_{98y2}~1). The underlying reason for this difference at high triangularity is not fully understood yet, but is most likely linked with the change of wall material and indicates that the gas injection itself is not the only cause of the reduced confinement factor. Also, in the low triangularity shape (δ~0.2), a minimum gas injection is now required, in contrast to the operation with JET-C. Figure 4b shows the behaviour of $P_{radbulk}/<n_e>2$ (representative of the impurity concentration in the discharge since Pradbulk scales as nenz and only weakly on T_e, like $T_e^{1/2}$ typically) as function of the gas bleed amplitude. Above 2.10^{22}D/s, the level of core radiation is equivalent to that with the carbon wall. But this level takes off by a factor 5 to 6 when the gas is lowered. In the lowest fuelling cases, the bulk radiation is in general higher than in equivalent pulses in the JET-C and the confinement factor H approaches sometimes 1, indicating that the H = 1 access operating space is strongly reduced with the JET-ILW (Figure 4a).

The discharge shown in figure 2 suggests that impurity peaking is occurring in the plasma core of the discharge thus enhancing the core radiation [18]. In ASDEX Upgrade, these events have been related to the strong neoclassical transport of high Z impurities in the plasma core [12]. To understand the relative weight between the source and the tungsten transport in the H-mode discharges, radiation peaking has been examined for H-mode discharges in relation with the tungsten source inferred from spectroscopy (photon flux of the 400.8 nm WI line) integrated over the whole bulk tungsten divertor tile. This has been done by selecting a dataset of pulse run at same Ip, BT (2.5MA, 2.7T), plasma shape (therefore identical λ_q according to the recent multi-machine scaling [19]) and same PNET range (from 12 to 14MW), i.e. same power flowing in the scrape-off layer. The spectroscopic data have been averaged over one second and therefore over typically 20 to 30 ELMs and averaged of the bulk tungsten tile surface (~1m^2) weighted by the toroidal wetted fraction (~0.7) to provide the total photon flux. Figure 5 shows that in the low triangularity shape the tungsten source averaged over ELM and inter-ELM phases decreases with the gas injection rate by typically a factor of 2 when the gas in quadrupled. Much less variation of the source is observed for the high triangularity discharge. This first analysis of the tungsten source, indicates that the strong radiation peaking observed at low gas fuelling is not only caused by the influx of tungsten induced by hot ions hitting the targets, but impurity transport in the core of the discharge is also playing a key role in the behaviour of the H-mode discharge in particular when the ELM frequency is not sufficiently high. Note that these discharges are not in a detached regime between ELMs; therefore the temperature at the outer strike point is expected to be well above 10eV.

The change of the wall composition is most likely at the origin of all the differences described above between the JET-C and JET-ILW. The absence of carbon as main divertor radiator could

lead to higher temperature in the JET-ILW divertor [20]. Bolometric reconstruction shows a strong reduction of the radiated power in the divertor outer region with the JET-ILW by typically a factor of 3 (Figure 6a and 6b) in otherwise identical plasma conditions (I_p, B_T, P_{IN}) and for identical upstream and pedestal density, as inferred from the high resolution Thomson scattering diagnostic. This could lead to higher conducted parallel power and thus different scrape-off layer temperature conditions. The neutral recycling, as measured from visible spectroscopy at the edge is also substantially altered with the JET-ILW as Be/W and C have not the same affinity to deuterium in term of retention and pumping [1]. A higher inter-ELM recycling is observed with the JET-ILW, increased by a factor 2 for similar deuterium puffing rate and NBI power conditions while the intra-ELM is strongly reduced. It has to be noted that the deuterium gas puffing rate is still an order of magnitude below the recycling neutral flux but its impact on the confinement appears stronger [1]. In addition, the lower observed Z_{eff} could play a role in the edge transport barrier and pedestal stability, which would be consistent with the observation made by the first nitrogen seeding experiments with the JET-ILW [21] and AUG results [3], where the H~1 could be recovered when injecting nitrogen gas which can radiate at the plasma edge.

3. DEVELOPMENT OF THE H-MODE BASELINE SCENARIO AT $I_P = 3.5$MA

On the basis of the first H-mode regime developments at 2.5MA/2.7T ($q_{95} = 3.5$), low shape ($\delta = 0.2$) baseline has been developed up to 3.5MA/3.2T ($q_{95} \sim 3$). This target provides an expansion of the operating domain to lower ρ^* and ν^* and thus interesting data for the study of ELM heat load, particle peaking and confinement scaling as it was done with the JET-C [22] in view of the extrapolation to ITER. In addition, high current operation has been the occasion to consolidate plasma operation techniques in a metallic wall environment and in particular the development of active protections of the components, plasma and HL transition landing and a controlled disruption using the mitigation valve [23].

As presented in the previous section, in contrast to the JET-C, even larger gas injection rate (up to 6 10^{22}e/s) had to be used at higher plasma current to stabilise the discharge and keep the ELM frequency above ~10 to 20Hz. In addition, strike point sweeping of about +/-6cm has been successfully applied over the bulk tungsten tile to mitigate the surface temperature tile below 1200°C and spread the power over several stacks of the bulk tungsten tile. Thanks to this, discharges have been successfully developed up to 3.5MA and β_N~1.4 with up to 26MW of NBI power for more than 5s duration and a Z_{eff} of 1.2-1.3 (figure 7). ICRH power has also been coupled successfully up to a level of 3.5MW. The resonance layer was located close to the magnetic axis and H minority (~5%) scheme used throughout this experiment. Electron heating (electron cyclotron heating and ion cyclotron heating) has been used in another metallic device, ASDEX Upgrade, to control the core impurity concentration and therefore the radiation level in the discharge [3]. Although an elevation of the core temperature and enhanced sawtooth activity are clearly observed in the ICRH phase in JET, there is no clear evidence yet that core ICRH heating had an impact on the high Z impurity

level indicating that higher level of ICRH power is probably required..

On the other hand, the ICRH power has been successful in the current ramp-up phase in L-mode and in the H-mode termination phase at the H to L transition. In this phase, the electron temperature could be increased up to 6-7keV using 4MW of ICRH coupled power with ~5% hydrogen minority and did help in preventing radiation collapse. To complement this picture, it should be noted here that in L-mode, the ICRH power has been correlated with an increased level of core radiation when compared to the identical level of neutral beam power [24]. This difference could originate from an undetermined source of tungsten when ICRH is applied. In the present high current H-mode discharges, it was not possible to determine the role played by this source in the total radiated power. In comparison high current scan with the same triangularity, the confinement is consistently lower by 20 to 30% at same plasma current, q_{95} and shape (figure 8). This has been achieved despite injecting in some cases more than 50% of power than the power threshold Pth from the scaling [25], which is equivalent to what had been done with the JET-C in similar conditions. Attempts to recover the confinement by lowering the gas injection and increasing PNET/Pth well above 2 while keeping the ELM frequency above 10Hz, have not succeeded in recovering more than 10% of the confinement. In the carbon wall, only low level of gas injection rate ($<1e^{22}$e/s) had been used, so a straight comparison with the Be/W wall is not possible. However figure 9 indicates for these types of discharges a correlation of the loss confinement with the gas injection in line with the equivalent discharges in the carbon wall. As a result, the ρ^* range are higher by typically 50% and 30% respectively with respect to similar discharges with the JET-C.

With the JET-ILW a lower fraction of the thermal and magnetic energy is radiated during the disruption. This results in a higher fraction of the energy to be conducted to the place facing components and also increases the current quench duration. The latter enhances the impulse exerted by the disruption on the vessel and could results in high vertical excursions of the vessel [26]. Extrapolation from intentional vertical displacement events at lower current, showed that in the JET-ILW baseline scenario at Ip = 3.5MA the absolute disruption force could exceed 600 Tonnes, higher than what one would get with the JET-C. The experiments to qualify the efficiency of the massive gas injection (MGI) on disruption have shown that the MGI increases the radiation and thus reduces the heat loads and forces to the level of those observed in the JET-C [20]. Given these results, the MGI has been used routinely in closed loop above a plasma current of 2.5MA. To trigger the MGI sensors based on the lock-mode signal and current quench detectors (detecting dI_p/dt or poloidal flux variations) [27] have been used. These trigger acted 67 times for current of 2.5MA and above. However these detectors are sometimes acting too late in particular when the discharge is showing high core radiation often leading to radiation collapse in the termination phase. To cover a broader range of disruption types, an engineering real time predictor has been designed [28] and tested in open loop during the high plasma current experiment. Based on a combination of classifier of 7 characteristic temporal signals, this predictor showed that almost 90% of the disruptions could have been predicted 30ms in advance of the disruption. As an example this predictor could have

acted and triggered the MGI on time in a 3.5MA disruption (Force: 320T) that was induced by the ingress of a tungsten into the plasma. Finally, it should be stressed that the use of the MGI has not affected significantly the breakdown of the next plasma with the JET-ILW nor the performance in the subsequent discharges [7]

In parallel to the development of the H-mode Baseline, JET has carried out dedicated experiment to investigate the H-mode in the ramp-up and ramp-down phase. The goal is to address the flux consumption and internal inductance (li) evolution in these phases in the JET-ILW environment and assess whether these phases could be limited by the poloidal field system of ITER, as it was done with the carbon wall in JET [29, 30, 31] and DIII-D [32].

In this type of experiment the current ramps are scaled to ITER using the resistive time ($\sim <T_e>^{3/2}.a^2$) as a guide, resulting in current ramp-up rates of typically 0.36 to 0.28MA/s. In the current ramp-up the range of internal inductance in ohmic and H-mode at the end of the current rise is comparable to that obtained. Furthermore, in H-mode, the flux consumption in the current rise is less than in the JET-C by typically 25%.

The current ramp-down phase has been investigated along the same guide lines for ramps of –0.14 to –0.5MA/s. Although li increases from 0.9 to 1.2 in H-mode, the increase is limited as long as the discharge stays in H-mode. These results are in line with those obtained with the JET-C and therefore confirm that even for the fastest ramp-down it is possible to maintain plasma vertical position and avoid any significant flux consumption in the ramp-down of ITER. In general no increase of the core radiation is observed in these experiments. The results are also giving confidence that the ramp-up/down of the baseline scenario can be integrated in the baseline scenario in JET and controlled within the poloidal field coils limits of ITER.

Finally, the H mode termination and landing at high plasma current has been developed. Because the JET-ILW has changed the radiation distribution towards higher plasma core radiation, switching off the power at termination as it was done with the JET-C often resulted in a radiative collapse and a disruption. This may be explained by the longer time of residence of heavy impurity in the plasma than light impurity. The use of electron heating up to 4MW of ICRH in the landing phase has been instrumental in mastering the landing of the H-L transition by increasing the electron temperature to 5 to 7keV and probably the anomalous particle diffusion processes. However, more dedicated experimental work is necessary to understand the physics processes associated with the back-transition and the external transport barrier collapse. The control of the HL transition remains an important challenge for ITER operation.

4. DEVELOPMENT OF THE ADVANCED INDUCTIVE H-MODE (HYBRID) SCENARIO UP TO β_N~3

The hybrid scenario has also been developed using as references the work carried out with the JET-C [33]. This scenario is traditionally characterised by its access to high normalised pressure (β_N>2.5) and no or infrequent sawteeth activity thanks to its “broad” q profile shape close to unity

as the main heating power is applied. This is achieved in JET using the so-called current overshoot technique [34] which helps keeping the central target q value (qo) close to unity and maximising the amount of current density at mid-radius, which has the effect to delay the occurrence of neoclassical tearing modes before the current diffuses.

For achieving such "non standard" q profiles, the impact of the metallic wall in the current on plasma current ramp up has been first examined experimentally. After the plasma breakdown and an X-point formation 1.4s later, the plasma current is ramped up to its plateau in X-point (as planned for ITER). The comparison with the JET-C shows that more gas had to be injected in this phase to achieve the same plasma density. Too low gas injection (equivalent to what was injected in the JET-C) resulted in the creation of a supra-thermal electron population (up to 5MeV as detected by γ-ray spectroscopy) and an increased tungsten level, which can lead sometimes to hollow temperature profile in the ramp-up phase [9]. With increased gas injection, the early central q profile at the X-point formation is much lower in the plasma core - typically 3 or 4 instead of 6 or 7 as measured by Motional Stark Effect (MSE) - than it was with the JET-C in similar conditions. This observation may have consequences for scenario requiring early control of the target q profile such as the advanced tokamak scenario. The advanced inductive scenario is less affected by this first phase since the main heating phase is usually set up more than several resistive times after the X-point formation.

Using this plasma initial phase, the hybrid scenario has been developed at low shape (δ~0.2-0.3) and high shape (δ~0.4) for q_{95}~3.7 at 1.7MA/2.0T and 2.0MA/2.3T, all using the Ip overshoot technique. In these discharges, β control by the neutral beam power has been used to set up the scenario target β_N between 2.5 and 3. In all cases, the outer strike point was on the divertor bulk tungsten tile. This was in general not the case with the JET-C where the plasma configuration had a more outward strike point position closer to the pumping louvers of the divertor.

Despite the change in divertor geometry, it appeared that the hybrid scenario could reproduce for about 2 to 3s similar global performance (H = 1.2-1.3 with β_N~3) achieved in the JET-C at both high and low triangularity. For the low triagularity plasmas, similar H factor than in JET-C is achieved but at higher volume average density and lower volume average temperature, suggesting that kinetic profiles are different than with the JET-C as we will discuss in section 5 of this paper. In both cases, moderate gas fuelling rate (~5 10^{21} D/s) is required to keep the discharge stable at 2MA with regard to the increase of core radiation peaking. The high frequency ELMs (>40Hz) and high (by more than a factor of 3) PNET power above the H-mode threshold may explain this. On the other hand, the quantity $P_{radbul}k/<n_e>2$ is in general higher with the JET-ILW by a factor of 2 to 3 even in the case of high H factors. Exactly as for the baseline scenario (see previous section) the core radiation is larger (by typically a factor of 3) and the divertor radiation smaller (more than x2) at similar electron density and temperature.

When achieved, the high performance (H~1.3, β_N~3) of the advanced inductive scenario with the JET-ILW is often rolling over when MHD occurs in correlation with strong core radiation

peaking. The MHD signature is similar to that of the JET-C, namely: m = 1/n = 1 continuous activity (with sometimes intermittent sawteeth) and 3/2 and 4/3 modes have been identified. The 4/3 mode is often accompanied by the (1, 1) mode. When a rational surface tears and an islands forms, their impact on the plasma performance is more profound and leads generally to core radiation peaking (as observed on the increased soft X-ray level) and the loss of performance caused by high Z impurities (figure 11). This is in contrast with the JET-C where such events led to moderate loss of confinement of typically 15% for a 3/2 mode and 5% for a 4/3 mode, the core radiation was much lower and the discharge did not terminate in radiative collapse. From these observations, it seems on one hand that the MHD in the hybrid scenario is changing dramatically the particle transport properties of the high Z impurities. On the other hand, the presence of impurities may also impact on the mode stability. This complex interplay between MHD and impurity transport is not yet clear nor is how different the q profiles with the JET-C and with the W-wall are from the MSE measurements. A further optimisation of the q target profile and its evolution might help in avoiding the occurrence of the mode and its consequences. Experimentally, more stable operation could indeed be successfully achieved by setting up a lower βN target with the control scheme (2.7 instead of 3.0). The lower achieved normalised pressure does help in these cases avoiding the triggering of tearing modes but is also accompanied with a performance penalty (H~1.1-1.2 instead of 1.3).

5. SCENARIO CONFINEMENT PROPERTIES WITH THE JET-ILW

The poor confinement observed in the baseline scenario in general and the performance close to their JET-C target achieved by the advanced inductive scenario are quite unexpected. It is therefore interesting to review the differences between these two scenarii. First of all, both scenario are H-modes but operated at very different normalised pressure ($\beta_N = 1.4$ and $\beta_N = 3.0$ respectively). However, the baseline and hybrid H-mode scenarios are not run with the same I_p, B_T and q_{95} and may have therefore different transport properties. In addition, so far, the scenarios have not been operated in the same plasma current range and with the same magnetic configuration, which would allow a more accurate comparison of their confinement with the poloidal βP. Both scenarii received about the same loss power than equivalent discharges with the JET-C. The baseline scenario with the JET-ILW has been operated with a loss power significantly above the H-mode power threshold Pth by a factor 1.5 to 2.0 and the hybrid scenario above the threshold, by typically a factor of 2.0 to 3.5. It should be noted here that the power threshold from Martin's scaling has been derived mostly with data from carbon devices and do not account for the subtraction of the bulk radiation. In addition, LH thresholds studies in JET [35] with the JET-ILW are also indicating that Pth could be lower than with the JET-C [36].

So, in what follows, the difference in confinement between the baseline and the hybrid scenarios is examined looking at core and pedestal kinetic profiles data. This is done making an extensive use of the high resolution Thomson scattering diagnostic for Te and ne [36] using a large database (270 pulses) of H-modes baseline and hybrid at both high and low triangularity. The pedestal temperature

and density are inferred from a tanh fit of the HRTS measurements. In most of the pulses studied here the core ion temperature and rotation could not be inferred from the charge exchange diagnostic in part because of the low signal over noise ratio resulting from the low carbon concentration with the JET-ILW. However edge/pedestal charge exchange data could be obtained and are showing a very similar ion and electron temperature ($T_e \sim T_i$) in all scenarios. Therefore at least for the pedestal, we can consider that the observations on electrons also hold for the ions.

The pedestal temperatures and densities are compared in terms of T_{eped}/I_p and $n_{eped}/n_{Greenwald}$ so that pulses of different current and field could be compared. In this way the curved lines on figure 12 are representing constant β_p lines. From this figure, the pedestal temperature for the baseline scenario (both low and high shape) is significantly lower (by typically 25 to 30% for an equivalent pedestal density) possibly because of the strong gas fuelling applied to these discharges in general. The hybrid scenario at low shape is also showing low pedestal temperature but also a higher electron density. As a result, the pedestal electron pressure is typically the same and the data points are lying on the same β_p = constant line. On the same figure, the hybrid at high shape has also a lower electron temperature with respect to the JET-C, whereas the density does not seem to compensate this loss completely and the electron pedestal pressure is lower by typically 10 To 20%. From these observations, it appears that the pedestal confinemnt in the hybrid scenario does not behave in the same way as in the JET-C [37].

Figure 13a and 13b are illustrating the differences in electron temperature and density profiles for both the baseline and the hybrid H-mode scenario in similar conditions of plasma current, toroidal field strength, input power and gas injection rate. It is interesting to note that for the high shape ($\delta = 0.4$), the density profiles are very similar for both the JET-ILW and the JET-C both in terms of absolute values and gradients. The presence of such a density gradient could be the drive for heavy impurity neoclassical inward diffusion observed in the discharges shown in section 2. With the low shape, the density profiles are much higher with the metallic wall as observed in other metallic machines and are still showing a significant gradient. This is particularly apparent in the hybrid H-mode. The core transport is often characterised by the temperature and density gradient length R/L_T and R/L_n. Because of the lack of ion temperature, only partial conclusions can be drawn from the core profile analysis of in the confinement zone ($0.4<\rho<0.7$). In particular, it is not possible to check how far these plasmas are from the critical gradients of ion temperature gradient (ITG) instability. The fact that for the high shape hybrid H-mode, the density profile is identical and the temperature profiles very close one with another within the measurements uncertainties, tend to suggest that the conditions are close to those achieved in the JET-C where the ITG was thought to be the dominant mode driving the turbulence. However, for the low shape hybrid H-mode, the differences are so large between the JET-C and the JET-ILW in terms of T_i/T_e and also Z_{eff} that a complete transport analysis with the ion temperature measurements would be required to check this point thoroughly. This also implies that the collisionality for the low shape hybrid H-mode is typically 2 times lower in the JET-C than in the JET-ILW. This observation may have important

consequence in the particle (and impurity transport) as describe in recent work [38] where it was shown that particle transport increases with increasing collisionality.

From these observations, there is evidence that the change of wall material has changed both the pedestal and core kinetic profiles and gradients mostly in low density (low shape plasmas) and therefore modified the transport properties of both the baseline and hybrid scenario but possibly in different ways. At this point of the research, the lack of ion temperature in the core does not allow a detailed transport analysis. In the case of discharges with thermal equilibration between ions and electrons, Ti~Te could be assumed (for example for high current discharges). However, it is known that the ion temperature gradient plays a significant role in impurity neoclassical transport [39] and such an assumption could lead to incorrect conclusions on the transport differences between the JET-ILW and the JET-C.

CONCLUSIONS

The recent experiments at JET with the new JET-ILW have made significant progress in the scenario integration with a relevant wall for ITER. The operating domain for the scenarios is significantly different. In particular the access to a confinement factor of H = 1 is seriously restricted. The requirement to control the transport of tungsten by the ELMs using gas injection has been shown to impact on the discharge confinement properties. In addition, the gas injection, has a significant impact on the W source in the H-mode regime. Although the W edge source and contamination in the core can be observed to vary with gas fuelling and PNET, the evidence is pointing towards the key role played by the high Z impurity transport. The lower Z_{eff} (~1.3) and lower radiation (and higher separatrix and target temperature) at the plasma edge in comparison to the carbon wall could also play a key role in the scrape off layer transport. The observation that part of the stored energy in the baseline H-mode can be recovered using nitrogen injection [21] is a signature that the link between the SOL and the core confinement does exist. Despite these limitations, H-mode baseline discharges could be achieved to a plasma current of 3.5MA using strong fuelling and this has helped to consolidate the operation of the H-mode regime in particular with the integration of the disruption active control using the MGI installed on JET.

At this point, it is not yet completely clear why the advanced inductive hybrid H-mode achieves similar H factor than in the JET-C. The kinetic profiles observation are indicating that both pedestal and core profiles in both low and high shape are significantly different, suggesting that the transport details across the plasma radius is also different than with the JET-C. The higher operating q_{95} (~4) and the level of plasma current (less than 2MA) so far used in this scenario could be beneficial. Therefore, future experiments aiming at developing the hybrid H-mode to higher current and therefore higher thermal and particle confinement and longer duration could behave in a different way. In addition, the MHD stability in these discharges has now become a key concern for the future because of its consequence on the impurity transport and energy confinement time. Continuous (1, 1) activity, for example, leads to radiation peaking and confinement degradation when it tears. Their effect is

much worse than with the carbon wall. For the future of the inductive advanced scenario (hybrid) in a metallic wall, this emphasizes the importance of q profile control to prevent the triggering of tearing modes. This also suggests that the presence in the plasma of high Z impurities eroded from the divertor should be minimised even before (i.e. in the current ramp-up L-mode phase) the discharges enters into the burning phase.

The JET-ILW has also motivated the integration of key scenario elements such as the use of the massive gas injection [23] for disruption mitigation, safe procedures for the landing of the H-mode and the study of the current ramp-up and –down flux consumption [29, 30]. The MGI has been instrumental in producing H-mode discharges at current up to 3.5MA in JET with the JET-ILW. Although disruption cannot be predicted with 100% confidence yet, the use of the MGI in closed loop and the reduction of its reaction time (by bringing the MGI valve closer to the plasma in future campaigns) could minimise the disruption consequences to the minimum required for safe operation of the tokamak. Nevertheless, the triggering of the MGI must be used in the last resort after all other landing strategies have been exhausted. In the last campaign, safe landing procedures against core radiation collapse have also been developed using ICRH heating in the H to L transition for example. The development of these elements and their integration in the plasma scenario remains an essential task for the preparation of safe operation of ITER scenario.

ACKNOWLEDGEMENT

This work was supported by EURATOM and carried out within the framework of the European Fusion Development Agreement. The views and opinions expressed herein do not necessarily reflect those of the European Commission.

REFERENCES

[1]. S. Brezinsek, et al., "Fuel Retention Studies with the JET ITER-Like Wall", submitted to Nuclear Fusion, 2013

[2]. G.F. Matthews et al 2011 Physica Scripta 2011 014001 doi:10.1088/0031-8949/2011/T145/014001

[3]. R. Neu et al., "Overview on plasma operation with a full tungsten wall in ASDEX Upgrade", Journal of Nuclear Materials, 2013, in press, http://dx.doi.org/10.1016/j.jnucmat.2013.01.006

[4]. B. Lipchutz et al., 2012 Nuclear Fusion **52** 123002

[5]. E. Joffrin et al Nuclear Fusion **45** (2005) 626-634

[6]. P. Mertens, Proceedings of the 24th IAEA Fusion Energy Conference San Diego, USA 8-13 October 2012, IAEA-CN-197, EX/P5-24

[7]. P.C. de Vries et al 2013 Nuclear Fusion **53** 053003

[8]. K. Krieger et al., Journal of Nuclear Material **438** (2013) S262

[9]. J. Mailloux, Proceedings of the 39th EPS Conference on Plasma Physics, Vol. **36**F, ISBN 2-914771-79-7, P1.092

[10]. J. Coenen, et al., Journal of Nuclear Material, **438** (2013) S139
[11]. J. Bucalossi et al., Proceedings of the 39th EPS Conference on Plasma Physics, Vol. **36**F, ISBN 2-914771-79-7, O3.106
[12]. R. Neu 2011 Plasma Physics and Controlled Fusion **53** 124040
[13]. T. Püetterich, Journal of Nuclear Materials, **415**, 334-339 (2011)
[14]. G. Saibene, 2002 Plasma Physics and Controlled Fusion **44** 1769
[15]. G. Van Rooij, et al., Journal of Nuclear Material, **438** (2013) S42
[16]. E. de la Luna, Proceedings of the 24th IAEA Fusion Energy Conference San Diego, USA 8-13 October 2012, IAEA-CN-197, EX/6-1
[17]. P. Lang, Proceedings of the 24th IAEA Fusion Energy Conference San Diego, USA 8-13 October 2012, IAEA-CN-197, EX/P
[18]. T. Puetterich, Proceedings of the 24th IAEA Fusion Energy Conference San Diego, USA 8-13 October 2012, IAEA-CN-197, EX/P3-15
[19]. T. Eich, Proceedings of the 24th IAEA Fusion Energy Conference San Diego, USA 8-13 October 2012, IAEA-CN-197, ITR/1-1
[20]. M, Groth, et al., "Impact of carbon and tungsten as divertor materials on the scrape-off layer conditions in JET", submitted to Nuclear Fusion 2013.
[21]. C. Giroud et al, 2013 submitted to Nuclear Fusion
[22]. I. Nunes et al Nuclear Fusion **53** (2013) 073020
[23]. M. Lehnen et al, 2011 Nuclear Fusion **51** 123010 and ., Proceedings of the 24th IAEA Fusion Energy Conference San Diego, USA 8-13 October 2012, IAEA-CN-197, EX/9-1
[24]. M. Mayoral et al., Proceedings of the 24th IAEA Fusion Energy Conference San Diego, USA 8-13 October 2012, IAEA-CN-197, EX/4-3
[25]. Y. Martin, Journal of Physics, Conference Series **123** (2008) 012033
[26]. P C de Vries et al 2012 Plasma Physics and Controlled Fusion **54** 124032
[27]. C. Reux et al., 27th Symposium on Fusion Technology (SOFT), Liege, Belgium 2012, P4.58
[28]. J. Vega et a,l 27th Symposium on Fusion Technology (SOFT) , Liege, Belgium 2012, O3A.4
[29]. A.C.C. Sips, 2009 Nuclear Fusion **49** 085015
[30]. G.M.D. Hogeweij et al 2013 Nuclear Fusion **53** 013008
[31]. I. Nunes et al., 38th EPS conference on Plasma Physics, Strasburg 2011, P4.106
[32]. G.L. Jackson et al 2008 Nuclear Fusion 48 125002 doi:10.1088/0029-5515/48/12/125002
[33]. E. Joffrin et al. Proceedings of the 23rd IAEA Fusion Energy Conference Daejeon, 11-16 October 2010, EXC/1-1, in: http://www-naweb.iaea.org/napc/physics/fec/fec2010/html/fec10.htm
[34]. J. Hobirk, 2012 Plasma Physics and Controlled Fusion **54** 095001
[35]. C. Maggi, Proceedings of the 39th EPS Conference on Plasma Physics, Vol. **36**F, ISBN 2-914771-79-7 O3.108
[36]. M.N.A. Beurskens et al., 2013 Nuclear Fusion **53** 013001

[37]. M. N. A. Beurskens et al., Proceedings of the 24th IAEA Fusion Energy Conference San Diego, USA 8-13 October 2012, IAEA-CN-197, EX/P

[38]. C. Angioni, et al., Nuclear Fusion **47** (2007) 1326.

[39]. M. Valisa et al., Nuclear Fusion **51** (2011) 033002

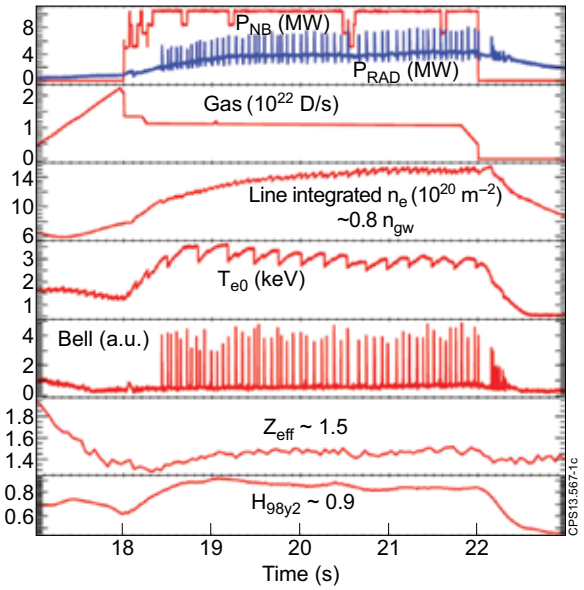

Figure 1: 2.5MA/2.7T (q_{95}=3.3) JET H-mode with the JET-ILW in the low shape magnetic configuration (δ=0.2). Note the fuelling rate necessary to make this scenario stable by keeping the ELM frequency typically above 10Hz to prevent strong core radiation peaking (see figure 2a and 2b).

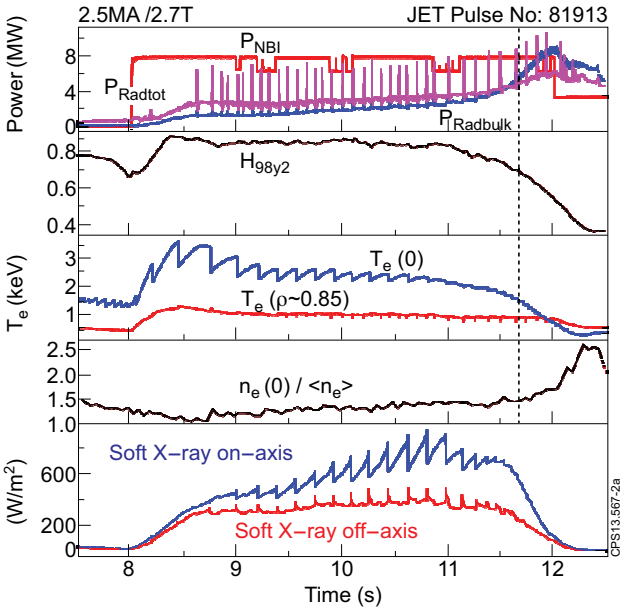

Figure 2: (a) Example of a core radiation increase in an H-mode with 2.0MA/2.2T (q_{95} = 3.3) in JET with the JET-ILW in the low shape magnetic configuration (δ = 0.2). Note the decreasing ELM frequency as the core radiation is increasing, the collapse of the central temperature and the loss of sawteeth, indicating a change of the core current profile shape. The loss of confinement is following the temperature decay and a significant peaking of the soft X-ray profile suggesting that high Z impurity have been transported to the plasma core. At the end of the discharge, the radiative power exceeds the total power and the density peaks dramatically. The dashed line indicates the time of the bolometry reconstruction shown in figure 2b.

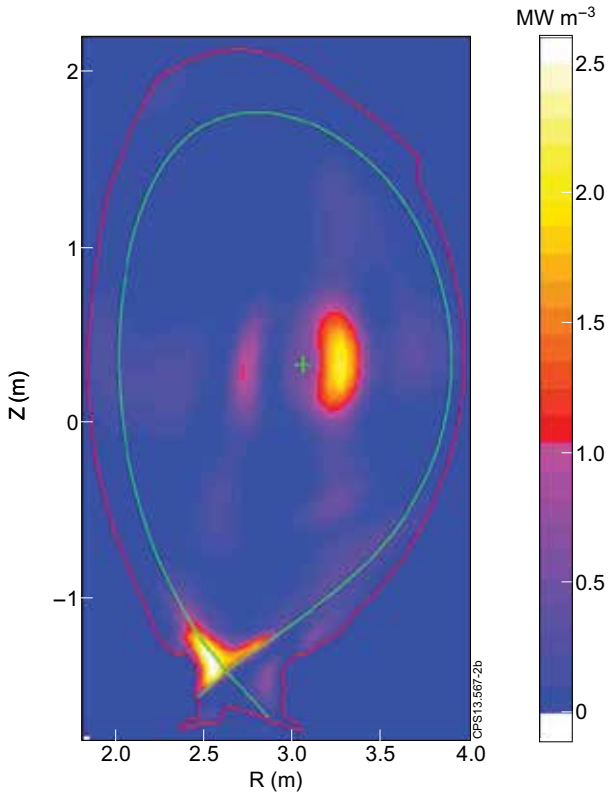

Figure 2: (b) Bolometry reconstruction for Pulse No: 81913 at 11.7s shown in figure 2a. Note the absence of any significant radiation in the outer divertor and the off-axis core radiation [16].

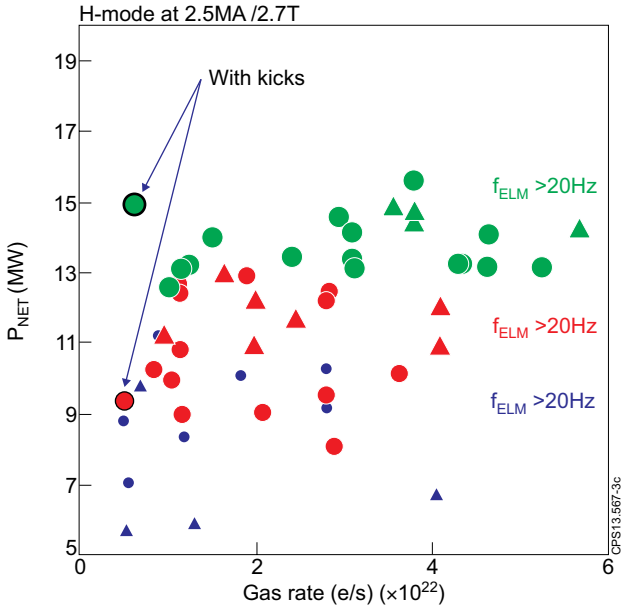

Figure 3: Net input power (=P_{IN}-$P_{RADBULK}$) versus the deuterium gas fuelling rate for both high triangularity pulses (triangles, δ = 0.4) and low triangularity (circles, δ = 0.2) type I ELMy H-mode at 2.5MA/2.7T with the ITER-like wall. The data are divided in 3 groups depending on their ELM frequency. Note that below P_{NET}~13MW, an ELM frequency above 20Hz can be achieved. Above ~9MW, an ELM frequency above 10Hz can be achieved. The low frequency H-modes (f_{ELM}<10Hz) are very often showing a high level of core radiation. The two dots pointed by the arrows have been achieved with vertical kicks (see [14]) suggesting that kicks could give access to the operation of the H-mode at low gas fuelling rate.

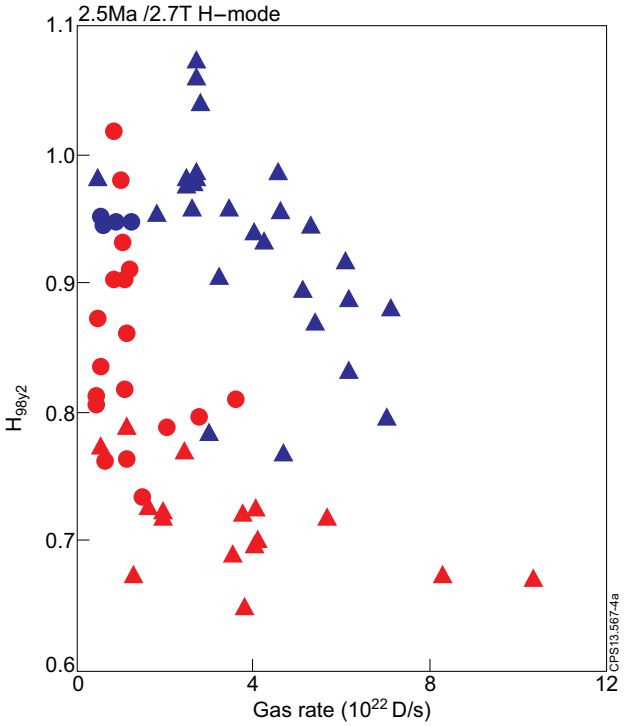

Figure 4: (a) H_{98y2} enhanced confinement factor (from the H_{98y2} scaling law) versus the gas rate for the same set of data than figure 3: blue with the JET-C and red with the W-wall. Circle (triangles) symbols are low (respectively high) triangularity magnetic configuration. Note that for the same plasma shape and same fuelling rate high triangularity plasma do not perform in the same way. With the W-wall, H = 1 could be reached only in a domain where the discharge is unstable with respect to core radiation (see figure 1 and 2).

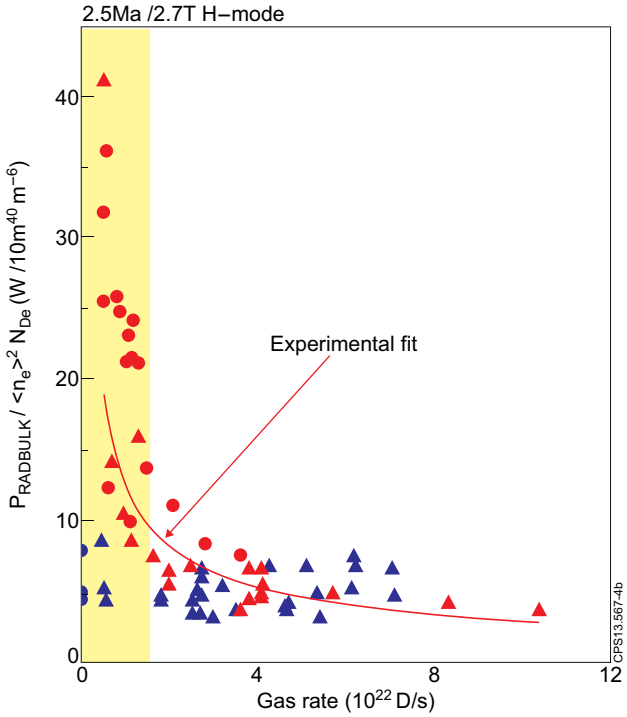

Figure 4: (b) Pradbulk normalised to the volume average density squared versus the gas rate for two datasets of H-mode discharges with I_p = 2.5MA and B_T = 2.7T, blue with the JET-C and red with the W-wall. Circle (triangles) symbols are low (respectively high) triangularity magnetic configuration. Note that with the carbon wall, the $P_{RADBULK}/<n_e>^2$ does not vary with the gas injection rate, whereas in the W-wall it increases strongly for gas fuelling rates typically below 2.10^{22} e/s.

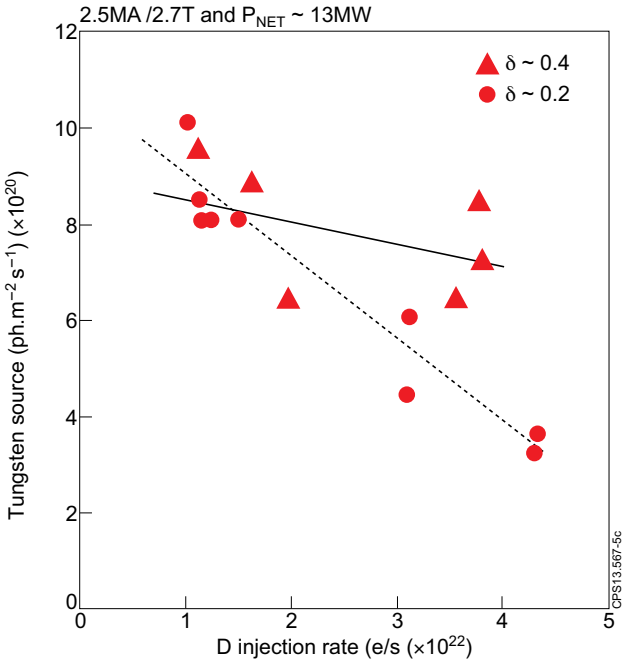

Figure 5: Tungsten source integrated over the whole bulk tungsten tile and over 1s as function of the gas injection for fixed P_{NET} power (using S/XB of 40). Note that for the low triangularity (dots, dashed line) the tungsten source decreases with gas injection by typically a factor of 2 when the gas rate is increased by a factor of 4 (see the dashed line linear square fit to the dots). On the other hand, the tungsten source does not decrease significantly in the case of the high shape (triangles, solid line).

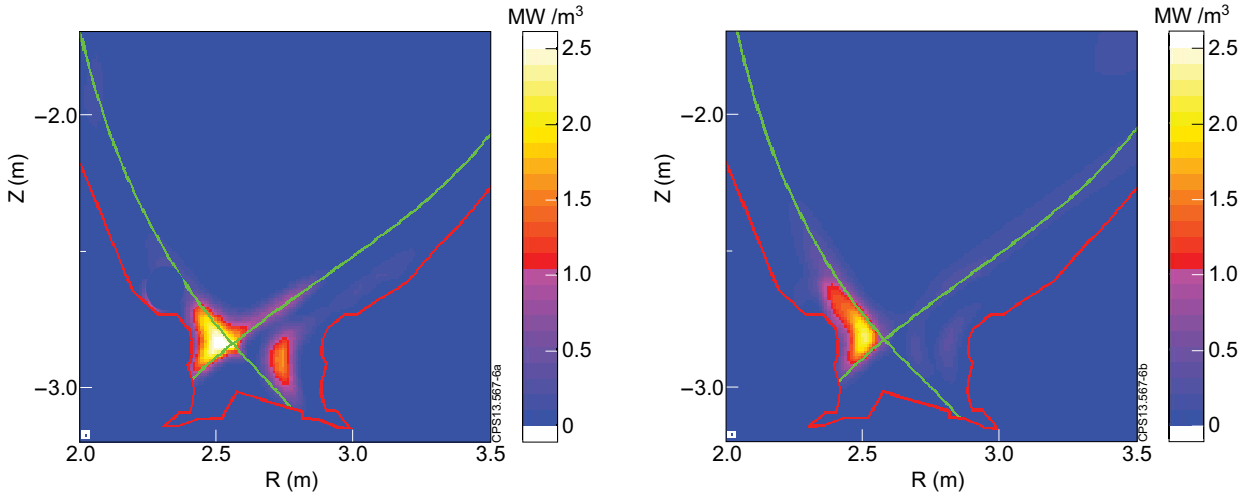

Figure 6(a) and 6(b): Comparison of the reconstructed radiated power from bolometry of one discharge with the JET-C (top) and one discharge with the JET-ILW (bottom). Please note that both discharges have the same upstream pedestal density according to the measurements by the high resolution Thomson scattering (HRTS) diagnostic. The radiation in the divertor area in particular on the outboard side is significantly lower with the JET-ILW (~factor of 3) than with the carbon wall.

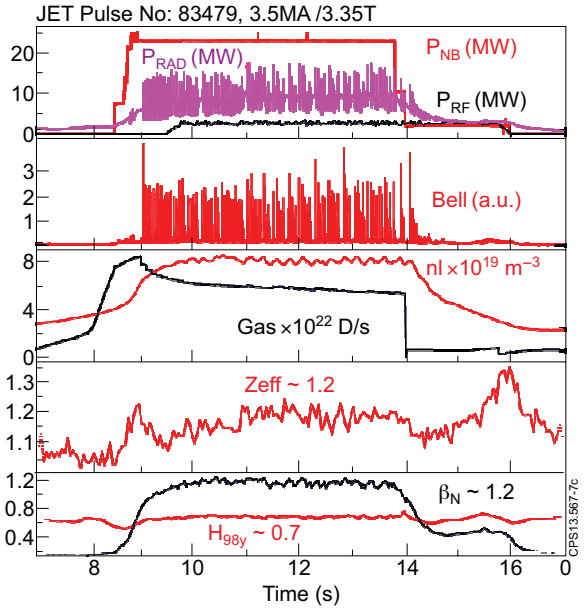

Figure 7: 3.5MA pulse run at JET with the JET-ILW. Note the strong D gas puffing rate and the plasma termination using a tail of ICRH and NBI power for 2s to allow for the decay of the radiation in the plasma core (shown in purple in the first box).

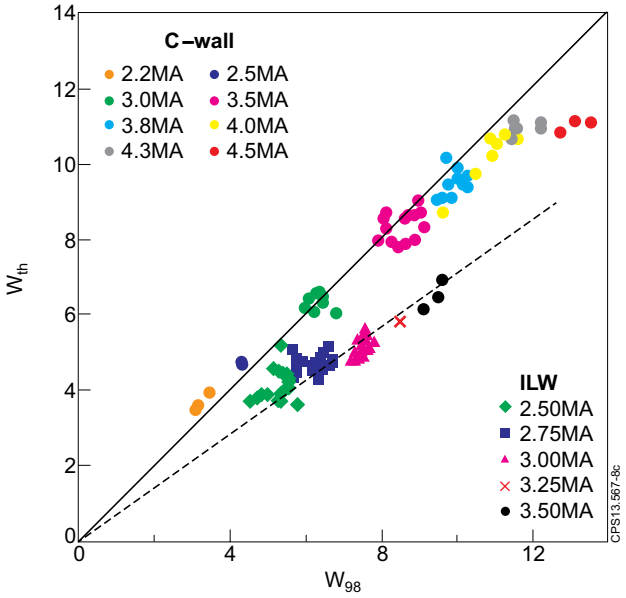

Figure 8: Comparison of thermal energy content with the predicted energy by H_{98y2} for a set of baseline H-mode at low shape in the carbon wall [22] and in the JET-ILW. The energy confinement with the JET-ILW is typically 20 to 30% lower than with the carbon wall.

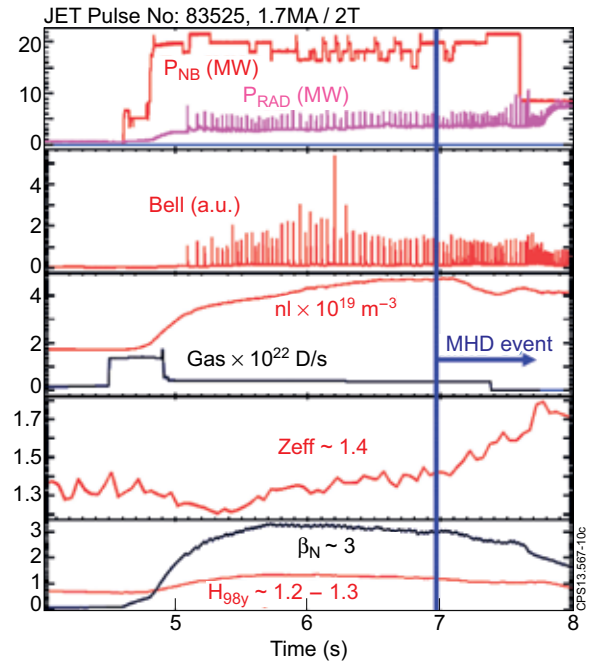

Figure 9: Confinement enhancement factor versus the gas injection rate for the high current discharges from 2.5MA to 3.5MA showing the loss of confinement with the JET-ILW. Note that the loss power over the power threshold has a ratio of 1.5 to 2 for all these cases.

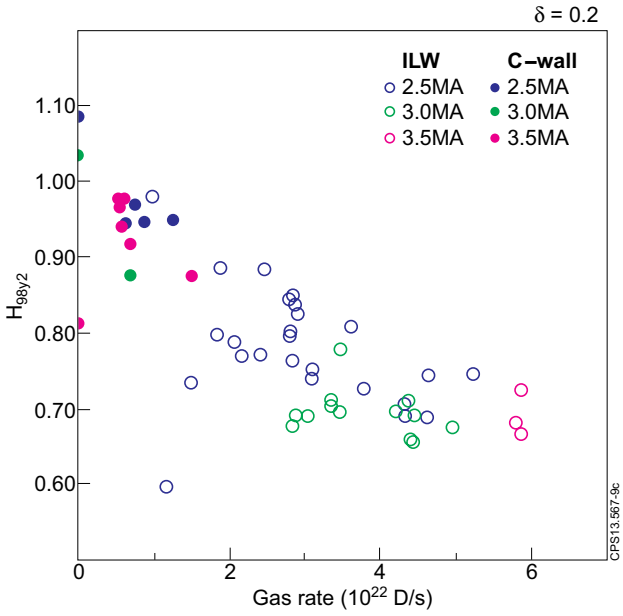

Figure 10: Advanced inductive (hybrid) pulse with δ = 0.2 run at JET at β_N~3 with the JET-ILW for ~2s. The performances are rolling over after 2s and core radiation increasing when the continuous (1, 1) activity becomes a magnetic island after 7s as indicated by the straight line (see also figure 10).

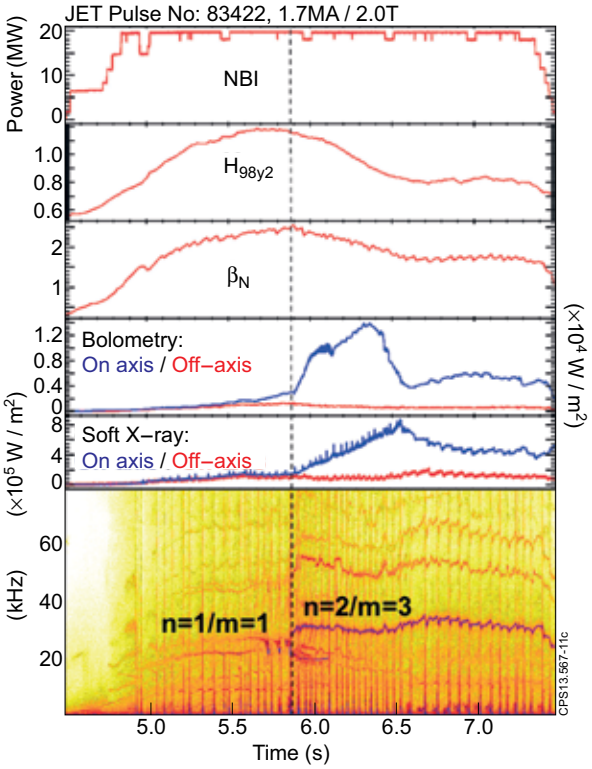

Figure 11: Example of the effect of tearing mode on the radiation in a typical hybrid discharge. The mode starts as a (1,1) that tears at 5.8s and produces an n = 2, m = 3 island. As observed on both soft X-ray and bolometry signals, radiations are strongly peaking at this time indicating that impurities have moved towards the plasma core and performance are rolling over dramatically from that point.

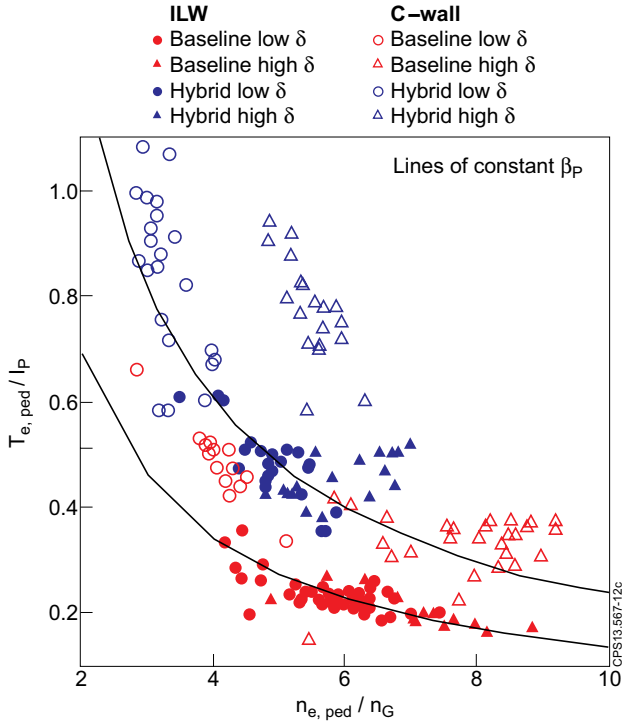

Figure 12: Pedestal difference in terms of Te_{ped}/I_p and ne_{ped}/n_G for the baseline H-mode (red) and the hybrid H-mode (blue). Open symbols with the JET-C and plain symbols with the JET-ILW. Triangles are high shape magnetic configuration, circle low shape. The continuous lines are representing iso-β_p. Typical error bar on the pedestal temperature and density measurement is +/–10%. With the JET-ILW the pedestal temperature has in general lower values for equivalent densities. Note also that the hybrid scenario at low shape is now operated with a larger density than in the JET-C.

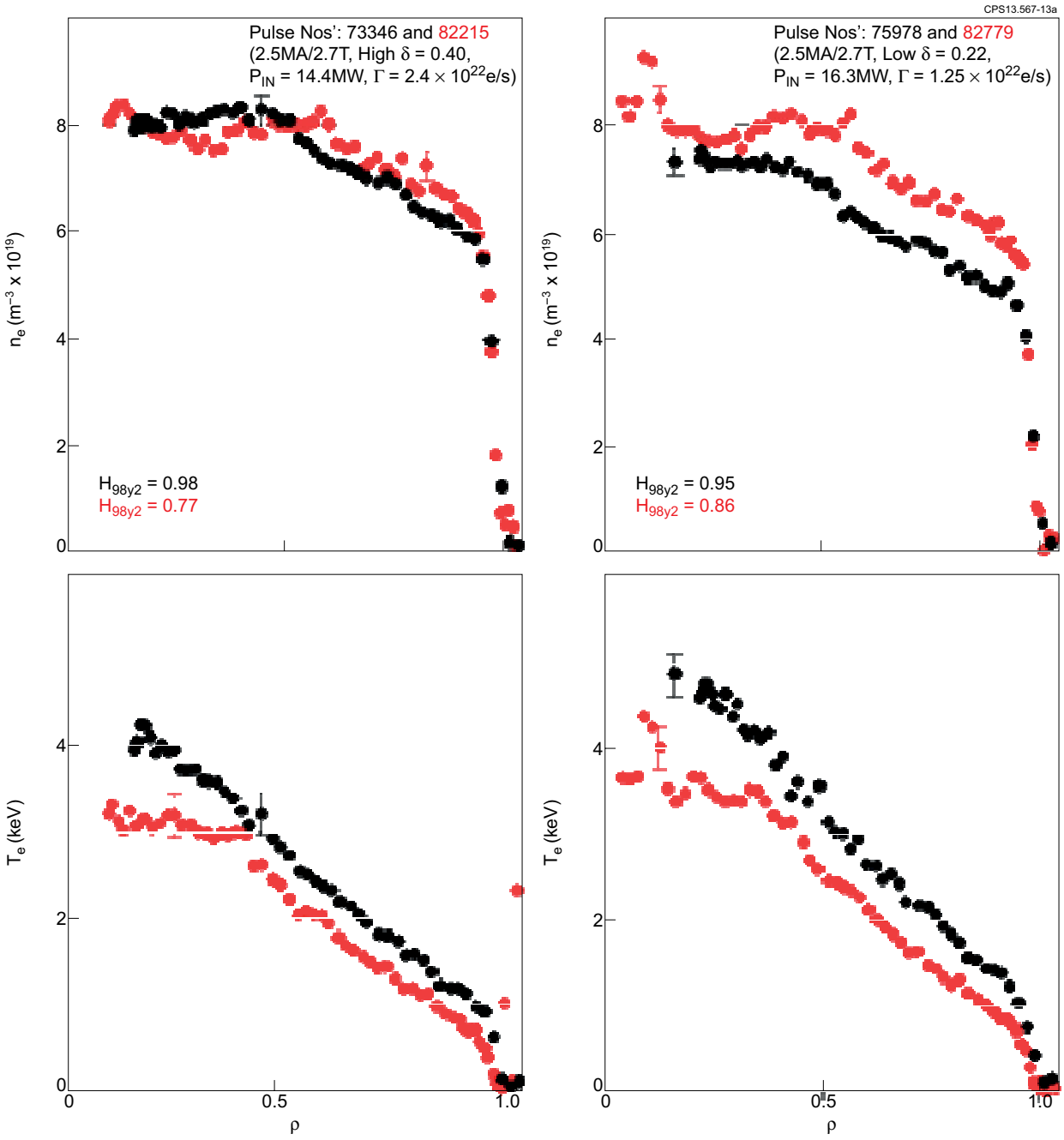

Figure 13: (a) Comparison of electron temperature and density profiles between JET-C (black) and JET-ILW (red) for the baseline H-mode scenario at high shape (right) and low shape (left) in identical conditions of input power and gas rate injection. For the high shape the density profile are almost identical but there exists a deficit in electron temperature. For the low shape, density is higher and the temperature significantly lower.

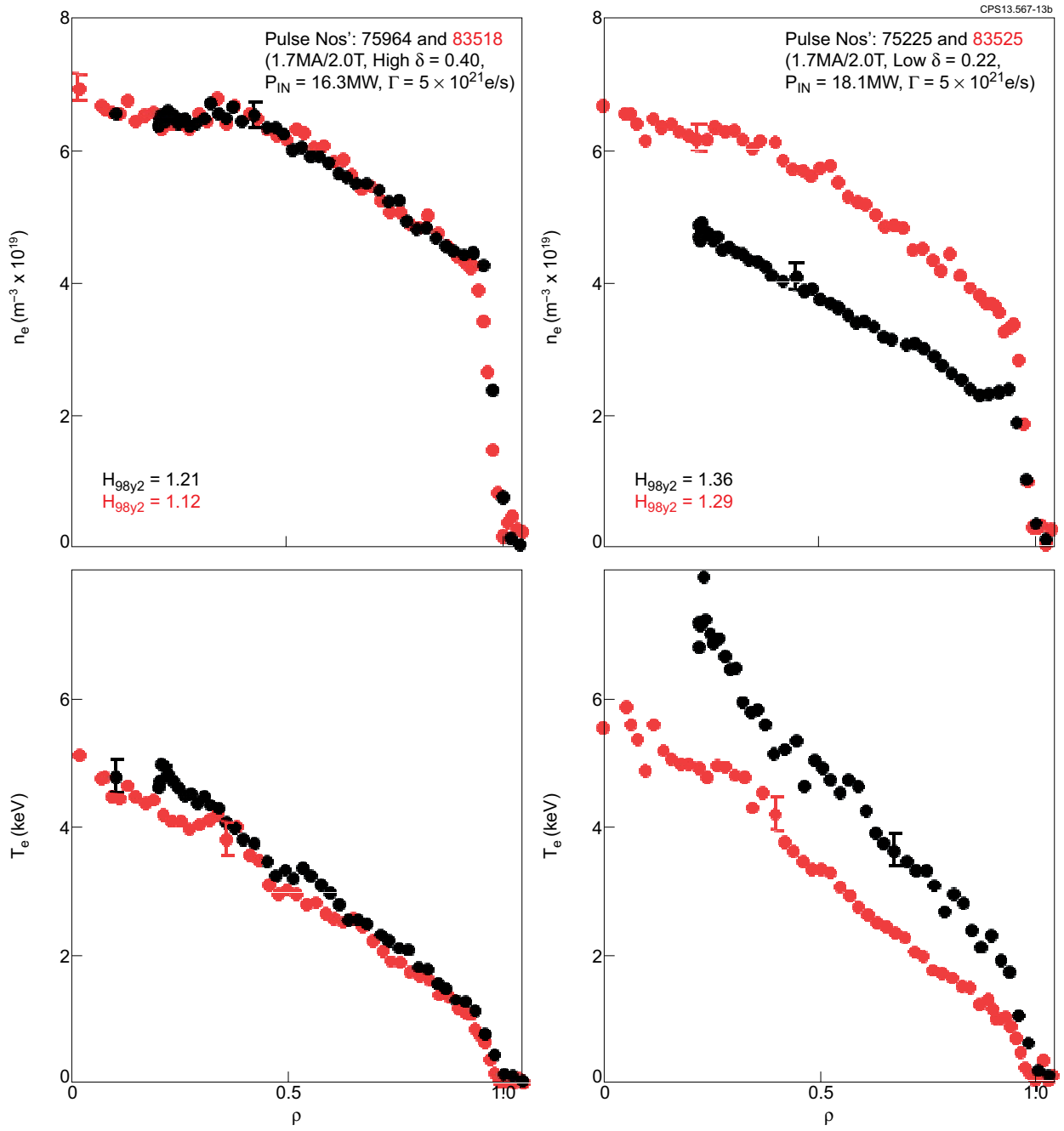

Figure 13: (b) Comparison of electron temperature and density profiles between JET-C (black) and JET-ILW (red) for the hybrid H-mode scenario at high shape (right) and low shape (left) in identical conditions of input power and gas rate injection. For the high shape the density profile are almost identical and the electron temperature very close one with another. At low shape, density is higher and but the temperature significantly lower, making the electron pressure almost identical (see figure 14).